JOINT PP AND PS ANISOTROPIC AVO INVERSION USING THE EXACT ZOEPPRITZ EQUATIONS

YIFEI BAO[1]*, JINGYI CHEN[1], XIAOBO LIU[2] and ZHENCONG ZHAO[1]

[1] Seismic Anisotropy Group, Department of Geosciences, the University of Tulsa, Tulsa, OK 74104, U.S.A. jingyi-chen@utulsa.edu
[2] School of Geophysics and Information Technology, China University of Geosciences, Beijing 100083, P.R. China.
** Present address: School of Sciences, Beijing University of Posts and Telecommunications, Beijing 100876, P.R. China.*

(Received December 13, 2020; revised version accepted July 21, 2021)

ABSTRACT

Bao, Y., Chen, J., Liu, X.B. and Zhao, Z.C., 2001. Joint PP and PS anisotropic AVO inversion using the exact Zoeppritz equations. *Journal of Seismic Exploration*, 30: 529-544.

With increasing complexity of the geological structure, the conventional amplitude variation with offset (AVO) inversion methods based on the approximate Zoeppritz equations are not suitable for the current direct hydrocarbon detection. The linearized approximations of the Zoeppritz equations work well under the conditions of weak contrast boundary and small incident angle, which not only restrict the scope of application but also reduce the accuracy of the inversion results. Furthermore, since the seismic anisotropy has been found in many regions of the Earth's subsurface, the assumption of isotropic elastic media cannot exactly describe the subsurface properties. Therefore, we develop an anisotropic AVO inversion method by replacing the approximate isotropic Zoeppritz equations with the exact isotropic Zoeppritz equations, and the Rüger's approximations are still used in the anisotropic perturbation part. In addition, we add the PS seismic data as a new constrained condition to improve the inversion results. In this study, we also obtain the analytical expressions of the derivatives of reflection coefficients with respect to unknown parameters (e.g., P- and S-wave velocities, density and Thomsen parameters: ε and δ). Given more parameters are required in anisotropic AVO inversion, the instability of the solution becomes a critical problem. We conduct the Marquardt method to enhance the stability during the inversion process. In this paper, we use a synthetic seismic data with ideal and noisy situations to verify the performance of the proposed AVO inversion algorithm. The final inversion results indicate that our new method works well to obtain the elastic parameters (density, P- and S-wave velocities) and Thomsen parameters.

KEY WORDS: exact Zoeppritz equations, transversely isotropy,
PP and PS reflection coefficients.

0963-0651/21/$5.00

INTRODUCTION

Seismic data can provide useful information for the hydrocarbon detection, especially it can generate the image of subsurface structure (Liu et al., 2012; Sun and Zhao, 2006; Russell, 2014). The amplitude variations with incidence angle (AVA) or amplitude variations with offset (AVO) inversion is commonly used to invert the reservoir properties effectively by utilizing seismic data (Buland and Omre, 2003; Hampson, 1991; Lu et al., 2018; Rutherford and Williams, 1989).

The fundament of the AVO inversion is the Zoeppritz equations that can relate the incidence angle with the seismic reflectivity. The Zoeppritz equations are a set of nonlinear functions with reference to the incidence angle and elastic parameters (P-wave velocity, S-wave velocity and density) that reveal the partitioning of seismic wave energy at a boundary between two different rock formations. Because the analytical solution of the exact Zoeppritz equations is difficult to obtain, the linearized approximate expressions of the Zoeppritz equations (Aki and Richards, 1980; Shuey, 1985) have been developed to calculate the seismic wave reflection and refraction coefficients easily in the conventional AVO inversion methods (Bortfeld, 1961; Li et al., 2005; Lu et al., 2018). However, these approximations are based on the assumptions of weak contrast at the interface and a small incidence angle. It is too hard to satisfy this assumption due to the complexity of geological structure. Thus, the seismic wave reflection and refraction coefficients that calculated by the approximate Zoeppritz equations will have tiny errors. After considerable iterations in the inversion process, these tiny errors will accumulate and lead to large deviations in the final inversion results.

Furthermore, as Thomsen (1986) indicates, seismic anisotropy widely exists in the earth's crust that can generate nonnegligible effect to seismic wavefields. Especially, the vertical transverse isotropy (VTI) medium is common in the reservoir rock (Backus, 1962; Carcione et al., 1991; Sidler and Holliger, 2010; Thomsen, 1986). However, the conventional AVO inversion methods focus on isotropic media, and may lead to incorrect inversion results (Castagna and Backus, 1993; Liu et al., 2012). Therefore, the presence of VTI can dramatically overcome the shortcomings of the conventional isotropic AVO inversion methods (Kim et al., 1993; Rüger, 1997; Wright, 1987).

Thomsen (1986) introduced the Thomsen parameters (ε and δ) to describe VTI media effectively, which means more parameters are required to calculate by the anisotropic AVO inversion. In the inversion processing, more parameters will lead to local minimum problem occurring more frequently (Lee et al., 2010; Lu et al., 2018). Considerable studies have focused on the Zoeppritz equations for transversely isotropic media. Daley and Hron (1977) proposed the exact formulas of the Zoeppritz equations for the transversely isotropic media. Banik (1987) introduced Thomsen parameters in the expression of P-wave reflection coefficient. While those equations are too intricate to use in an anisotropic AVO inversion. Different from previous researches, Rüger's (2002) present linearized PP and PS-wave reflection coefficient expressions for the VTI medium (known as Rüger approximations) which are much easier to use in anisotropic AVO inversion and can provide precise results (Booth et al., 2016; Lu et al., 2018).

In this paper, we develop a new Anisotropic AVO inversion method. We first obtain the isotropic reflection coefficients calculated by the exact isotropic Zoeppritz equations, then get the analytical solutions of the derivatives of reflection coefficients with respect to unknown parameters (e.g., P- and S-wave velocities, density and Thomsen parameters) (Liu et al., 2012; Bao et al., 2019). Due to Rüger's linearized formulas clearly describe the isotropic and anisotropic effects on reflection coefficients, we employ the anisotropic part of Rüger approximations as the anisotropic perturbation term, and calculate the derivatives of anisotropic reflection coefficients with respect to unknown parameters in the anisotropic media. Moreover, adding the PS-wave reflection coefficients to the conventional PP-wave AVO inversion can effectively reduce multiple solutions and solve the local minimum problem (Auger et al., 2003; Veire and Landrø, 2006). To avoid the unstable solution, we also adopt the Marquardt method (Marquardt, 1963). We use a truncated Taylor series expansion regarding the model unknown parameters to generate the updating formula for the inversion, and apply the least-squares method to establish the objective function. Finally, we test our proposed method with the synthetic seismic data and compare the AVO inversion results (P- and S-wave velocities, density and Thomsen parameters) with the conventional method (Aki and Richards' (1980) approximation). The model study indicates that our proposed method can feasible and precisely invert the rock properties in anisotropic media.

THEORY

Reflection coefficients and gradients

We add an anisotropic perturbation term on the isotropic term to calculate the reflection coefficients in the VTI medium. It can be expressed as:

$$R = R_{iso} + R_{anis}, \tag{1}$$

where R_{iso} and R_{anis} denote the isotropic and anisotropic parts, respectively.

The isotropic part of the reflection coefficients is generated by the exact Zoeppritz equations. It is written as:

$$R_{iso} = A^{-1}B,$$

where

$$A = \begin{pmatrix} \cos\alpha & -\sin\beta & \cos\alpha' & \sin\beta' \\ \sin\alpha & \cos\beta & -\sin\alpha' & \cos\beta' \\ \cos 2\beta & -\eta_1 \sin^2\beta & -\rho_{21}\eta_2 \cos 2\beta' & -\rho_{21}\eta_3 \sin 2\beta' \\ \eta_1^2 \sin 2\alpha & \eta_1 \cos 2\beta & \rho_{21}\dfrac{\eta_3^2}{\eta_2}\sin 2\alpha' & -\rho_{21}\eta_3 \cos 2\beta' \end{pmatrix}, \tag{3}$$

$$B = \left(\cos\alpha \quad -\sin\alpha \quad -\cos 2\beta \quad \eta_1^2 \sin 2\alpha\right)^T, \tag{4}$$

$$R_{iso} = \left(R_{PP} \quad R_{PS} \quad T_{PP} \quad T_{PS}\right)^T. \tag{5}$$

In eqs. (3) and (4), α and β indicate the incidence angles of the P- and S-waves, respectively. α' and β' denote refraction angles of P- and S-waves, respectively. $\eta_1 = V_{s1}/V_{p1}$, $\eta_2 = V_{p2}/V_{p1}$, $\eta_3 = V_{s2}/V_{p1}$ and $\rho_{21} = \rho_2/\rho_1$. V_P and V_S are the P-and S-wave velocities, respectively, ρ is the density of the medium. We use subscripts “1” and “2” to represent the upper and lower layers, respectively.

For the anisotropic part of eq. (1), we apply the Rüger’s reflection coefficient equations (Rüger, 2002) to calculate the PP and PS reflection coefficients, which are written as:

$$\begin{cases} R_{PP}^{anis} = \frac{1}{2}(\delta_2 - \delta_1)\sin^2\alpha + \frac{1}{2}(\varepsilon_2 - \varepsilon_1)\sin^2\alpha\tan^2\alpha \\ R_{PS}^{anis} = \left[\left(\frac{V_P^2}{2(V_P^2 - V_S^2)\cos\beta} - \frac{V_P V_S \cos\alpha}{2(V_P^2 - V_S^2)}\right)(\delta_2 - \delta_1)\right]\sin\alpha \\ \quad + \left[\frac{V_P V_S \cos\alpha}{(V_P^2 - V_S^2)}(\delta_2 - \delta_1 + \varepsilon_1 - \varepsilon_2)\right]\sin^3\alpha \\ \quad - \left[\frac{V_P^2}{(V_P^2 - V_S^2)\cos\beta}(\delta_2 - \delta_1 + \varepsilon_1 - \varepsilon_2)\right]\sin^3\alpha \\ \quad + \left[\frac{V_S^2}{2(V_P^2 - V_S^2)\cos\beta}(\delta_2 - \delta_1)\right]\sin^3\alpha \\ \quad + \left[\frac{V_S^2}{(V_P^2 - V_S^2)\cos\beta}(\delta_2 - \delta_1 + \varepsilon_1 - \varepsilon_2)\right]\sin^5\alpha \end{cases} . \tag{6}$$

Here, ε and δ are known as Thomsen parameters; ε describes the fractional difference between the vertical and horizontal P-wave velocities, and δ describes the variation of P-wave velocity with incidence angle in near-vertical propagation. The V_P and V_s are the vertical (symmetry-axis) velocities of the P- and S-waves, respectively:

$$\begin{cases} V_P = \frac{1}{2}\left(V_{P1} + V_{P2}\right) \\ V_S = \frac{1}{2}\left(V_{S1} + V_{S2}\right) \end{cases} . \tag{7}$$

Based on eq. (1), the gradients of reflection coefficients can be written as:

$$\frac{\partial R}{\partial m} = \frac{\partial R_{iso}}{\partial m} + \frac{\partial R_{anis}}{\partial m} = \frac{\partial R_{iso}}{\partial m_{iso}} + \frac{\partial R_{anis}}{\partial m_{iso}} + \frac{\partial R_{anis}}{\partial m_{anis}} , \tag{8}$$

where the model parameter vector m can also be divided into isotropic and anisotropic parts, respectively. The isotropic part includes the elastic parameters: P- and S-wave velocities, the medium density, and the anisotropic part includes Thomsen parameters: ε and δ. Since Thomsen parameters are only related to the anisotropic term, we can ignore the partial derivatives of the isotropic term with respect to the Thomsen parameters.

Based on eq. (2), we can obtain the partial derivatives of the reflection coefficients by calculating the partial derivative equations of matrices ***A*** and ***B***. The gradients of isotropic part with respect to the elastic parameters can be written as:

$$\frac{\partial R_{iso}}{\partial m_{iso}} = -A^{-1}\frac{\partial A}{\partial m_{iso}}R_{iso} + A^{-1}\frac{\partial B}{\partial m_{iso}}. \tag{9}$$

From eqs. (8) and (9), we can obtain the gradients of reflection coefficients

$$\frac{\partial R}{\partial m} = -A^{-1}\frac{\partial A}{\partial m_{iso}}R_{iso} + A^{-1}\frac{\partial B}{\partial m_{iso}} + \frac{\partial R_{anis}}{\partial m_{iso}} + \frac{\partial R_{anis}}{\partial m_{anis}}. \tag{10}$$

Anisotropic AVO inversion

We first establish the joint PP and PS objective function *F*, which can be written as:

$$F(m) = w\left\|R_{PP} - D_{PP}\right\|^2 + (1-w)\left\|R_{PS} - D_{PS}\right\|^2, \tag{11}$$

where $m = (V_P, V_S, \rho, \varepsilon, \delta)$. R_{PP} and R_{PS} respectively are the synthetic PP and PS-wave reflection coefficients of the given model parameter vector *m*, which are generated by eq. (1). D_{PP} and D_{PS} are the real PP and PS wave reflection coefficients, respectively. We use the weight factor *w* to qualify the PP and PS data. *w* ranges from 0 to 1. The higher the quality of the data, the larger the weight. If both the PP and PS data have the same quality, *w* is 0.5. *w* will be 1 if only PP data are applied for the inversion.

Then, we use the truncated Taylor series expansion for R_{PP} and R_{PS} to build the updating formula of the inversion, which is written as:

$$R_{PP/S}(m_k + \Delta m) \approx R_{PP/S}(m_k) + \nabla R_{PP/S}(m_k)\Delta m, \tag{12}$$

where m_k is the parameter vector for the *k*-th iteration, and $\Delta m = (\Delta V_P, \Delta V_S, \Delta\rho, \Delta\varepsilon, \Delta\delta)$ is the update for the current parameter vector.

Let $G_{PP/S} = \nabla R_{PP/S}(m_k)$, we substitute eq. (12) into eq. (11):

$$F(m) = w\left\|(R_{PP} + G_{PP}\Delta m) - D_{PP}\right\|^2 + (1-w)\left\|(R_{PS} + G_{PS}\Delta m) - D_{PS}\right\|^2 . \qquad (13)$$

According to the least-squares method, eq. (13) can be written as:

$$\frac{\partial F(m)}{\partial \Delta m} = w\left\|(R_{PP} - D_{PP})^T G_{PP} + G_{PP}\Delta m\right\|^2 + (1-w)\left\|(R_{PS} - D_{PS})^T G_{PS} + G_{PS}\Delta m\right\|^2 = 0. \qquad (14)$$

Therefore, the update parameter vector Δm can be derived as:

$$\Delta m = [wG_{PP}^T G_{PP} + (1-w)G_{PS}^T G_{PS}]^{-1} \cdot [wG_{PP}^T (R_{PP} - D_{PP}) + (1-w)G_{PS}^T (R_{PS} - D_{PS})]. \qquad (15)$$

We update our model iteratively until the update vector reaches a satisfactory minimum.

While the solution of eq. (15) is unstable, because the singular matrix will appear in this equation occasionally. Here, we conduct the Marquardt (1963) method to avoid the instability during inversion. Eq. (15) becomes:

$$\Delta m = [wG_{PP}^T G_{PP} + (1-w)G_{PS}^T G_{PS} + \xi I]^{-1} \cdot [wG_{PP}^T (R_{PP} - D_{PP}) + (1-w)G_{PS}^T (R_{PS} - D_{PS}) + \xi I], \qquad (16)$$

where $\boldsymbol{I}$ is an identity matrix and ξ denotes a real constant that depends on the precision requirement.

Since we carry out the inversion with multiple incidence angles, we let θ_i indicates the i-th incidence angle, and R_n indicates the reflection coefficients of the n-th layer. The gradients of reflection coefficients G can be given as

$$G = \begin{pmatrix} \frac{\partial R_1(\theta_1)}{\partial m_1} & \cdots & \frac{\partial R_1(\theta_i)}{\partial m_1} & \frac{\partial R_1(\theta_1)}{\partial m_2} & \cdots & \frac{\partial R_1(\theta_i)}{\partial m_n} \\ \vdots & & \vdots & \vdots & & \vdots \\ \frac{\partial R_n(\theta_1)}{\partial m_1} & \cdots & \frac{\partial R_n(\theta_i)}{\partial m_1} & \frac{\partial R_n(\theta_1)}{\partial m_2} & \cdots & \frac{\partial R_n(\theta_i)}{\partial m_n} \end{pmatrix}. \qquad (17)$$

The zero-matrix elements are neglected.

To improve the inversion accuracy, we introduce a mean shift method to constrain the inversion results. After several iterations, we can generate an elastic parameter model that is close to the prior model by extrapolating from the well model. We calculate the mean values of each model, if the ratio between the mean values is large, then this ratio is used to scale the inverse model to improve its proximity to the prior model.

We also apply the PS to PP time-alignment processing technique in this study. Due to the use of a joint objective function in the AVO inversion, we should ensure the PS time is aligned with PP time by compressing PS time. To do this, the PS events need to match to the PP events from the same geologic strata with the help of well and synthetic data.

NUMERICAL EXAMPLES

In order to validate our method, we carry out two numerical examples. For both examples (with and without noises), we use a five-layer 1D model as the true model (shown in Table 1). The contrast of rock properties at each interface is high. We calculate the PP and PS reflection coefficients based on eq. (1) with the true model. Then, we calculate the synthetic PP and PS reflection coefficients with an initial model. The incidence angles are from 5^0 to 40^0 with the interval of 5^0, the sample rate is 1ms, and no multiples are considered in the tests.

Table 1. Rock properties of the five-layer model.

Thickness(m)	V_P(m/s)	V_S(m/s)	ρ(g/cm^3)	ε	δ
100	1980	808	2.01	0.25	0.2
80	2200	1260	2.2	0.21	0.13
60	2440	1340	2.31	0.13	0.19
60	2660	1480	2.4	0.3	0.24
150	1980	808	2.01	0.25	0.2

Example 1

We carry out the forward calculations of PP and PS reflection coefficients without noises. Since both PP and PS data are high quality, we set *w* is 0.5. The synthetic PP and PS seismograms are shown in Fig. 1, which are generated through the convolution of the reflection coefficients and the Ricker wavelet with the dominant frequency of 30 Hz. We change the polarity of PS-wave to match with PP-wave to ensure the PS reflection time correlates with PP reflection time.

Two different inversion methods are applied to invert P- and S-wave velocities, density and Thomsen anisotropy parameters in this test. One is based on the exact PP and PS reflection coefficients, and another is based on PP and PS reflection coefficients calculated by the Aki and Richards' approximation (Aki and Richards, 1980).

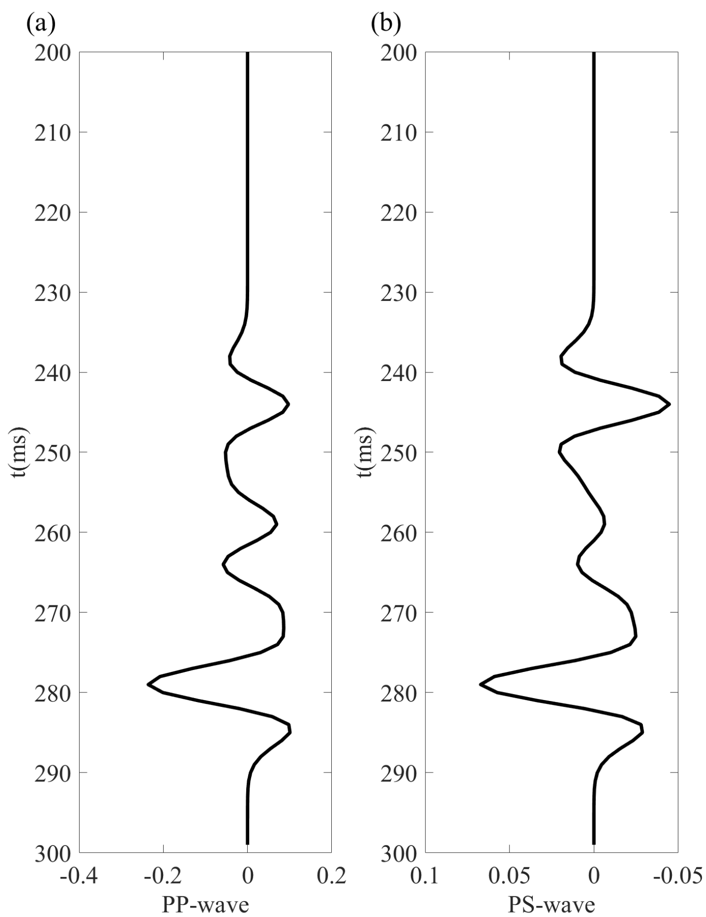

Fig. 1. Synthetic PP and PS seismograms in PP time domain; (a) PP-wave without noise, (b) PS-wave without noise. To match the PP-wave, the PS-wave data are compressed to PP time, and the polarity is reversed.

After several iterations, the inversion results are shown from Fig. 2 to Fig. 6 for P- and S-wave velocities, density, as well as Thomsen parameters ε and δ, respectively. As those figures shown, although there are strong contrasts in the true model, our new method based on the exact isotropic Zoeppritz equations can provide better results (velocities, density and Thomsen anisotropy parameters) than the Aki and Richards' approximation method. In addition, on can observe that the inverted P- and S-wave velocities and Thomsen parameters match the true model better than the inverted density because density shows more sensitivity to amplitudes (Lines, 1998; Du and Yan, 2013).

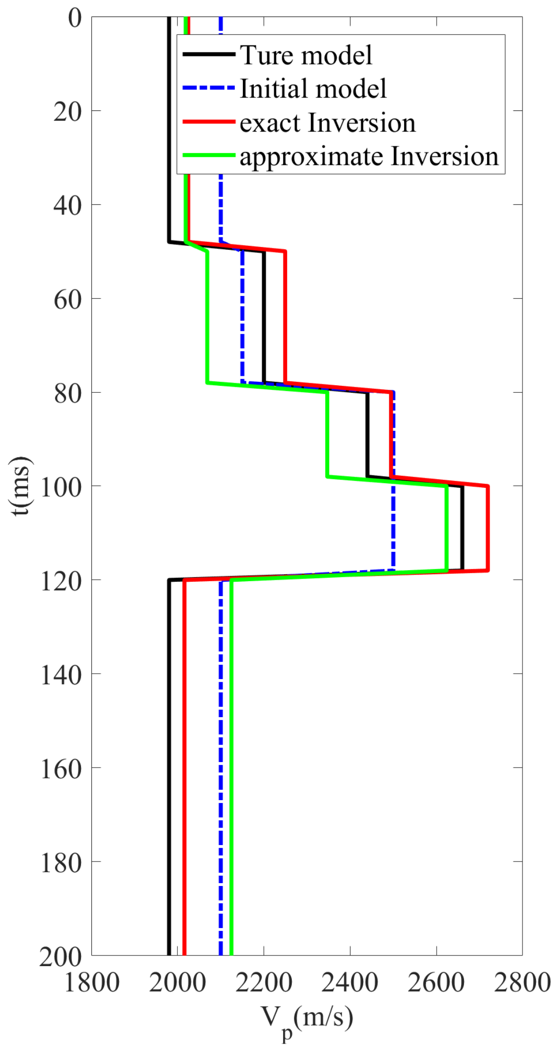

Fig. 2. Inversion result for P-wave velocity. The solid black line is the true model, blue dash line is the initial model. The solid red line is the inversion result by our proposed method and solid green line is the result using Aki and Richards' approximation.

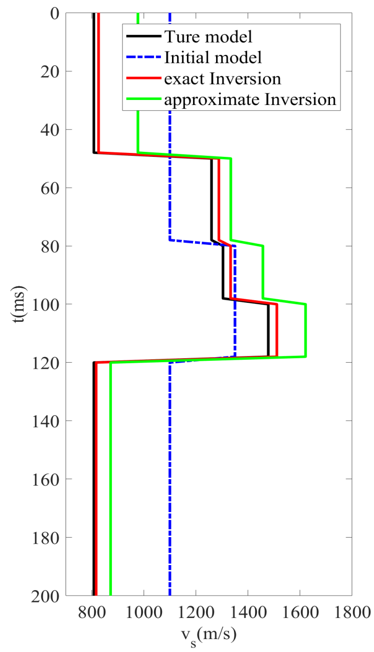

Fig. 3. Inversion result for S-wave velocity. The solid black line is the true model, blue dash line is the initial model. The solid red line is the inversion result by our proposed method and solid green line is the result using Aki and Richards' approximation.

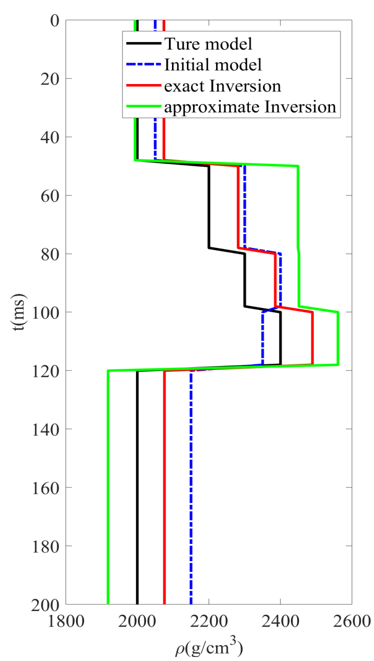

Fig. 4. Inversion result for density. The solid black line is the true model, blue dash line is the initial model. The solid red line is the inversion result by our proposed method and solid green line is the result using Aki and Richards' approximation.

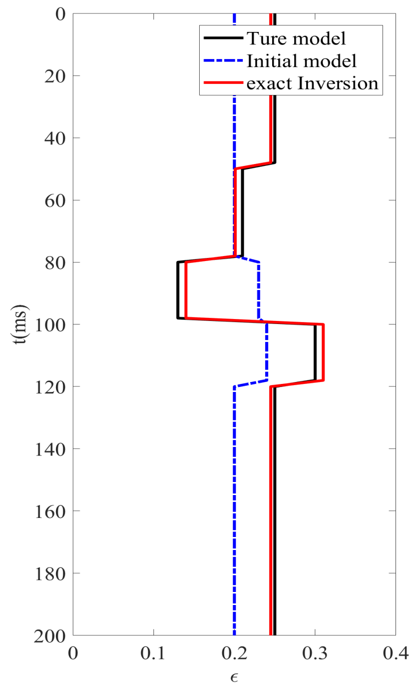

Fig. 5. Inversion result for Thomsen parameter ε. The solid black line is the true model, blue dash line is the initial model. The solid red line is the inversion result by our proposed method.

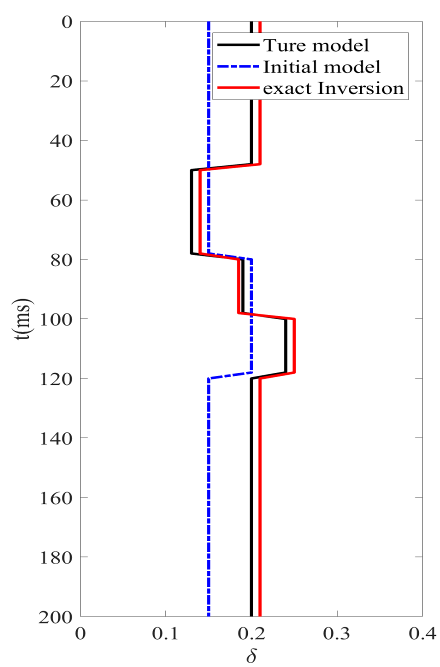

Fig. 6. Inversion result for Thomsen parameter δ. The solid black line is the true model, blue dash line is the initial model. The solid red line is the inversion result by our proposed method.

Example 2

In this study, we take into account the effects of noises. The accuracy of inversion is highly dependent upon the noise level. Fig. 7 shows the PP and PS wave signals with different random noise levels (15% and 5%). Based on the different noise levels, we give them different weights *w*.

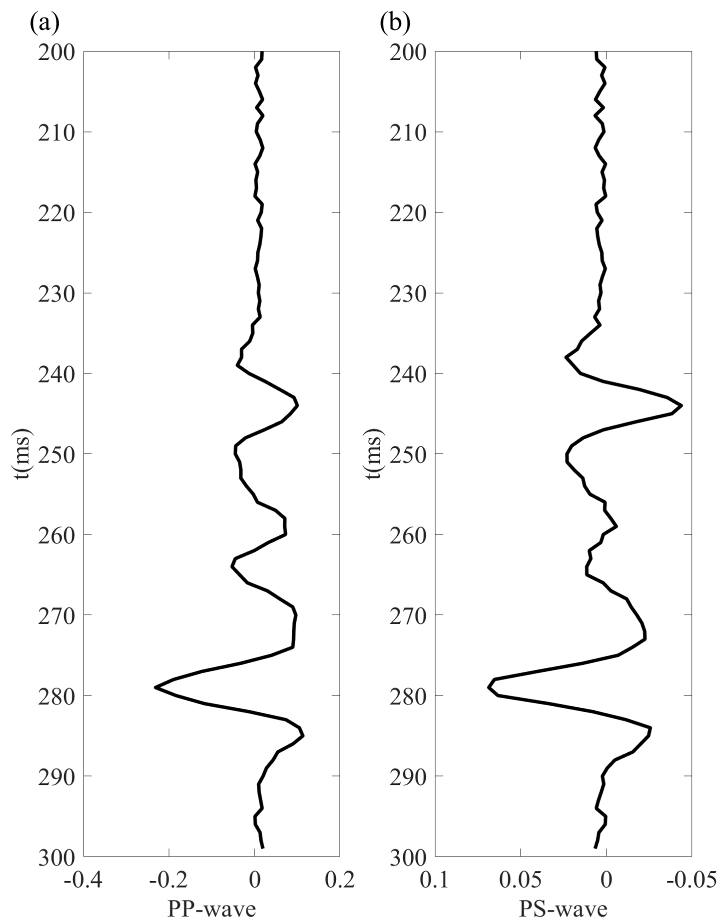

Fig. 7. Synthetic PP and PS seismograms in PP time domain; (2) PP-wave data with 15% random noise, (b) PS-wave data with 5% random noise. To match the PP-wave, the PS-wave data are compressed to PP time, and the polarity is reversed.

Fig. 8 shows the inversion results with only apply PP data. Obviously, the noise has a strong impact for the final model, which is not very close to the true model. Then, we combine PP and PS data to carry out the AVO inversion. Due to the low noise level of PS data, we give PS data with a larger weight in the inversion. The results are shown in Fig. 9. One can observe that the final model is much closer to the true model than the results shown Fig. 8.

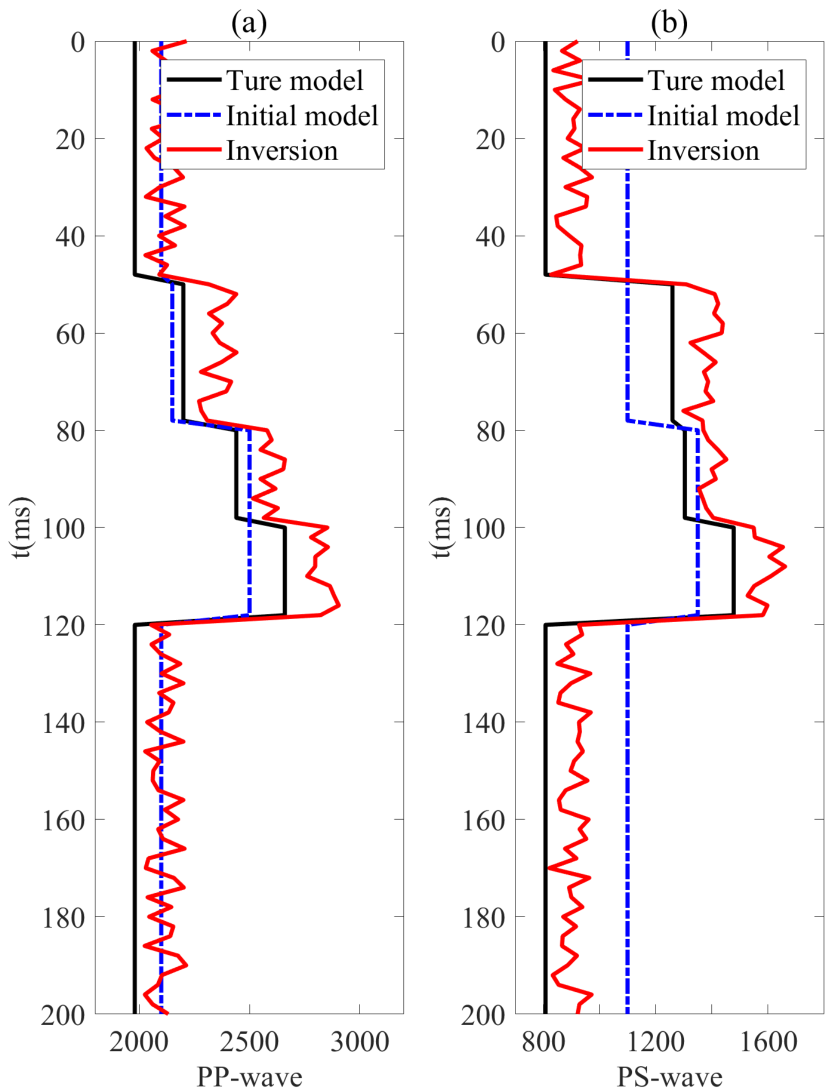

Fig. 8. Inversion results with only PP data: (a) P-wave velocity, (b) S-wave velocity. The solid black line is the true model, blue dash line is the initial model. The solid red line is the inversion result.

CONCLUSIONS

We successfully implemented the anisotropic AVO inversion after obtaining seismic reflection coefficients by the exact Zoeppritz equations and Rüger's expression in anisotropic media. The synthetic tests verified that our proposed method can deal with high-contrast interfaces of geological models, and provide more accurate inversion results (velocities, density and Thomsen anisotropy parameters) than the Aki and Richards' approximation.

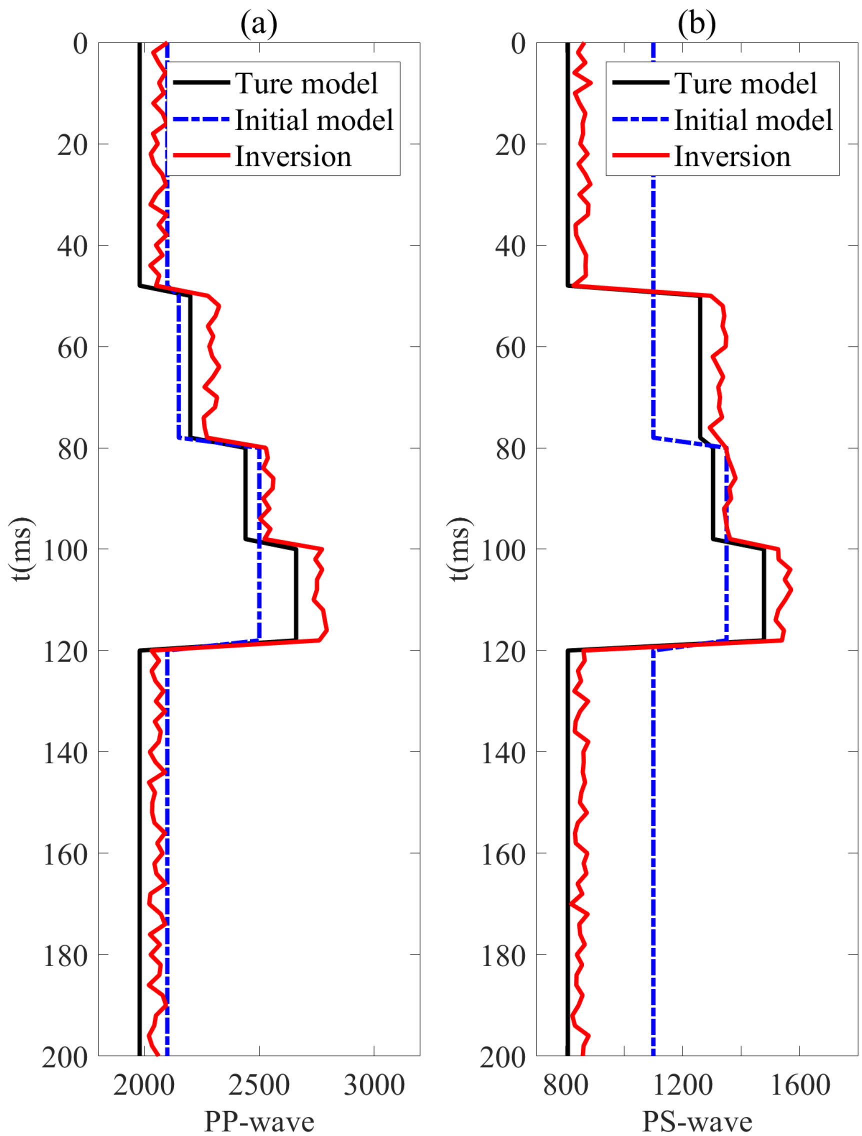

Fig. 9. Inversion results with the joint PP and PS data: (a) P-wave velocity, (b) S-wave velocity. The solid black line is the true model, blue dash line is the initial model. The solid red line is the inversion result.

REFERENCES

Aki, K. and Richards, P.G., 1980. Quantitative seismology: Theory and Methods. WH Freeman and Co., San Francisco.

Auger, E., Virieux, J. and Zollo, A., 2003. Locating and quantifying the seismic discontinuities in a complex medium through the migration and AVA analysis of reflected and converted waves: An application to the Mt. Vesuvius volcano. Geophys. J. Internat., 152: 486-496.

Backus, G.E., 1962. Long-wave elastic anisotropy produced by horizontal layering. J. Geophys. Res., 67: 4427-4440.

Booth, A.D., Emir, E. and Diez, A., 2016. Approximations to seismic AVA responses: Validity and potential in glaciological applications. Geophysics, 81(1): WA1-WA11.

Bortfeld, R., 1961. Approximations to the reflection and transmission coefficients of plane longitudinal and transverse waves. Geophys. Prosp., 9: 485-502.

Buland, A. and Omre, H., 2003. Bayesian linearized AVO inversion. Geophysics, 68: 185-198.

Carcione, J.M., Kosloff, D. and Behle, A., 1991. Long-wave anisotropy in stratified media: A numerical test. Geophysics, 56: 245–254.

Castagna, J.P. and Backus, M.M., 1993. Offset-dependent Reflectivity - Theory and Practice of AVO Analysis. SEG, Tulsa, OK.

Daley, P.F. and Hron, F., 1977. Reflection and transmission coefficients for transversely isotropic media. Bull. Seismol. Soc. Am., 67: 661-675.

Hampson, D., 1991. AVO inversion, theory and practice. The Leading Edge, 10: 39-42.

Liu, X.B., Liu, F.P., Meng, X.J. and Xiao, J.Q., 2012. An accurate method of computing the gradient of Seismic Wave Reflection Coefficients (SWRCs) for the inversion of stratum parameters. Surv. Geophys., 33: 293-30.

Lu, J., Wang, Y., Chen, J. and An, Y., 2018. Joint anisotropic amplitude variation with offset inversion of PP and PS seismic data. Geophysics, 83(2): N31-N50.

Marquardt, D.W., 1963. An algorithm for least-squares estimation of nonlinear inequalities. J. Soc. Industr. Appl. Mathemat., 11: 431-441.

Ostrander, W.J., 1984. Plane-wave reflection coefficients for gas sands at non-normal angles of incidence. Geophysics, 49: 1637-1648.

Rüger, A., 2002. Reflection coefficients and azimuthal AVO analysis in anisotropic media. Society of Exploration Geophysicists.

Shuey, R.T., 1985. A simplification of the Zoeppritz equations. Geophysics, 50: 609-614.

Thomsen, L., 1986. Weak elastic anisotropy. Geophysics, 51: 1954-1966.

Veire, H.H. and Landrø, M., 2006. Simultaneous inversion of PP and PS seismic data. Geophysics, 71(3): R1-R10.